Resonance Raman and UV−Vis Spectroscopic Characterization of FADH• in the Complex of Photolyase with UV-Damaged DNA†

Johannes P. M. Schelvis,*,‡ Meghan Ramsey,§ Olga Sokolova,‡ Celia Tavares,‡ Christine Cecala,‡ Katelyn Connell,§ Stacey Wagner,§ and Yvonne M. Gindt§

Department of Chemistry, New York University, 31 Washington Place, Room 1001, New York, New York 10003 and Department of Chemistry, Lafayette College, Easton, Pennsylvania 18042

Received: January 25, 2003; In Final Form: June 11, 2003

Escherichia coli photolyase uses blue light to repair cyclobutane pyrimidine dimers which are formed upon irradiation of DNA with ultraviolet (UV) light. *E. coli* photolyase is a flavoenzyme which contains a flavin adenine dinucleotide (FAD) in its active site and a 5,10-methenyltetrahydrofolate (MTHF) as a light-harvesting pigment. In the isolated enzyme, the FAD cofactor is present as a stable neutral radical semiquinone (FADH•). In this paper, we investigate the interaction between photolyase and UV-damaged DNA by using resonance Raman and UV−vis spectroscopy. Substrate binding results in intensity changes and frequency shifts of the FADH• vibrations and also induces electrochromic shifts of the FADH• electronic transitions because of the substrate electric dipole moment. The intensity changes in the resonance Raman spectra can be largely explained by changes in the Raman excitation profiles because of the electrochromic shift. The size of the electrochromic shift suggests that the substrate binding geometry is similar to that of oxidized FAD in reconstituted photolyase. The frequency changes are partially a manifestation of the vibrational Stark effect induced by the substrate electric dipole moment but also because of small perturbations of the hydrogen-bonding environment of FADH• upon substrate binding. Furthermore, differences in the resonance Raman spectra of MTHF-containing photolyase and of an MTHF-less mutant suggests that MTHF may play a structural role in stabilizing the active site of photolyase while comparison to other flavoproteins indicates that the FAD cofactor has a strong hydrogen-bonding protein environment. Finally, we show that the electrochromic shift can be used as a direct method to measure photolyase−substrate binding kinetics.

Ultraviolet (UV) light irradiation can lead to a variety of DNA damage, for example, strand breaks and dimerization of adjacent pyrimidine bases.[1] The most common UV-photoproduct is the cyclobutane pyrimidine dimer (CPD) with an abundance of about 80%.[2] It has been shown that these dimers cause a bend in duplex DNA which hinders transcription and replication.[3−5] If this damage is not repaired, it can lead to mutagenesis, carcinogenic growth, and cell death.[6,7]

Photolyases are flavoenzymes that belong to the class of blue-light photoreceptors and that repair this DNA specific damage in a light-driven, electron-transfer mechanism.[8−10] Photolyases share a common cofactor; flavin adenine dinucleotide (FAD) forms the active site of the enzyme in its reduced hydroquinone form ($FADH^-$).[8,9] Two other flavin redox states are possible: the neutral radical semiquinone (FADH•) which can be converted to $FADH^-$ in the presence of light, and the oxidized FAD cofactor (FAD_{ox}) which cannot be activated under physiological conditions. Most photolyases also contain a second chromophore which apparently functions as a light-harvesting pigment. Two molecules have been identified as the second chromophore: 5,-10-methenyltetrahydrofolate polyglutamate (MTHF) and 8-hydroxy-5-deazaflavin. *Escherichia coli* photolyase is a 55 kDa, monomeric enzyme which contains MTHF as its second chromophore.[11−13] *E. coli* photolyase was the first to be successfully overexpressed making it the most-studied photolyase.[14]

It has been proposed that monomerization of the CPD photoproduct is initiated from the singlet excited state of $FADH^-$, from which an electron is transferred to the CPD, followed by reductive cleavage of the dimer, and electron-transfer back to the FAD cofactor.[8,15] This photorepair process takes less than 10 ns. In the isolated enzyme, the FAD cofactor is present as FADH• which is stable under aerobic conditions.[12,16] FADH• can be converted to its active form by light-driven electron transfer from a nearby tryptophan (Trp) residue to FADH• to form $FADH^-$.[8,17] The initial electron-transfer step takes 30 ps, and a chain of Trp residues has been proposed to be involved with Trp306 as the terminal electron donor.[17,18] In the absence of exogenous electron donors, the back electron transfer occurs on the millisecond time scale.[16,17,19] Although the electron-transfer processes in *E. coli* photolyase are reasonably well understood, much less is known about the interactions between the enzyme and its substrate.

The interaction between photolyase and UV-damaged DNA has mainly been studied by biochemical techniques.[20] It was shown that *E. coli* photolyase has a very high affinity ($K_d = 10^{-9}$ M) for DNA containing a CPD photoproduct while its affinity for undamaged DNA is almost 5 orders of magnitude lower, and it binds equally well to damaged single-stranded (ss) and double-stranded (ds) DNA.[21,22] The enzyme protects a 6−8

† This work was supported by startup funds from New York University (J. P. M. S.), by a New York University Research Challenge Fund Grant (O. S.), and the Lafayette College EXCEL Scholars Program (M. R., K. C., and S. W.)

* To whom correspondence should be addressed. Tel: (212) 998 3597; fax: (212) 260 7905; e-mail: hans.schelvis@nyu.edu.

‡ New York University.

§ Lafayette College.

10.1021/jp034209l CCC: $25.00
Published on Web 10/14/2003

base pair region surrounding the dimer, and the phosphodiester bond 5′ and three phosphodiester bonds 3′ to the dimer are important for high-affinity binding.[23−25] Photolyase also contains several highly conserved residues on its surface which have been proposed to belong to a common recognition site.[20,24,26] A major breakthrough was the determination of the crystal structure of *E. coli* photolyase.[26] The most prominent feature of the structure is a large cavity originating at the protein surface and ending near the FAD cofactor buried within the protein's interior. Subsequent structure determinations of *Anacystis nidulans* and *Thermus thermophilus* photolyase have shown that this cavity and other active-site features are conserved in photolyases from different organisms.[26−28] It has been proposed that the cavity forms the substrate-binding site and that the CPD photoproduct flips out of the DNA duplex into the cavity in van der Waals contact with the FAD cofactor.[26] This mechanism is also known as dinucleotide flipping. Although attempts to obtain cocrystals of photolyase with UV-damaged DNA have been unsuccessful, the structure of *T. thermophilus* photolyase with thymine shows that one-half of a CPD photoproduct can bind in the substrate cavity, supporting the proposal that the CPD binds in the cavity.[28]

Further support for the dinucleotide-flipping model and insight into the photolyase−substrate complex have been obtained from biochemical, computational, and spectroscopic studies.[29−36] The computational studies show that the photolyase cavity can accommodate a CPD lesion, but they predict a range of CPD to FAD distances from 3 to 9 Å.[29−32] Recent ENDOR and electronic absorption experiments have estimated the CPD to FAD distance to be >6 Å and between 5.5 and 8 Å, respectively.[33,35] The latter estimate indicates that the CPD has to bind in the cavity and is based on the electrochromic shift of the electronic transitions of the oxidized FAD cofactor induced by the electric dipole moment of the CPD.[35]

A recent fluorescence study of substrate binding to oxidized photolyase with 2-aminopurine containing DNA also supports the dinucleotide-flipping model.[36] The spectroscopic investigations of photolyase−substrate interactions have been performed on photolyase reconstituted with oxidized FAD and on an MTHF-less E109A mutant of photolyase containing $FADH^{\bullet}$.[33−36] Such modifications may perturb the protein conformation near the active site and affect the photolyase−substrate interactions. To avoid these potential complications, experiments on the wild-type enzyme as isolated are desirable. Furthermore, recent experiments have provided evidence in support of CPD-binding in the substrate cavity,[29−36] but the mode of damage recognition by photolyase remains a matter of debate, that is, whether photolyase recognizes the bend in dsDNA and induces dinucleotide flipping upon binding to the substrate or binds to the CPD when it is outside the DNA duplex during a base-opening phase.[5,23,28−30,32,36] To address this important issue, the development of a direct method to measure the binding kinetics of photolyase to UV-damaged DNA will be necessary.

In this paper, we use resonance Raman and UV−vis spectroscopy to investigate the interactions between the active site in unmanipulated photolyase and UV-damaged DNA. Resonance Raman spectroscopy is an excellent tool to study flavoproteins, and information about the structure of the flavin molecule and its interactions with the protein environment can be obtained.[37,38] The resonance Raman spectrum of photolyase is slightly different from that of the MTHF-less, E109A mutant suggesting that the mutation may have perturbed the active site.[39] The high quality of our resonance Raman spectra allows us to detect intensity changes and small frequency shifts upon addition of substrate to photolyase. The intensity changes can be largely explained by the electrochromic shift of the $FADH^{\bullet}$ transition dipole moments induced by the electric dipole moment of the CPD. The frequency shifts are associated with changes in hydrogen bonding to $FADH^{\bullet}$ but are also partially related to the vibrational Stark effect because of the substrate dipole. Furthermore, the electrochromic shift of $FADH^{\bullet}$ is similar to that of FAD_{ox} indicating a similar substrate−binding geometry in both the unmanipulated and FAD^{-}reconstituted enzymes and supporting the binding of CPD in the substrate cavity.[35] Finally, we show that the electrochromic shift of the $FADH^{\bullet}$ absorption bands induced by the CPD electric dipole moment provides a direct method to measure the kinetics of photolyase binding to UV-damaged DNA.

Materials and Methods

Cell Growth and Harvest. *E. coli* strain pMS969 was a generous gift from Drs. A. Sancar and G. T. Babcock. The *E. coli* cells were grown and harvested using the procedure outlined previously with the following modifications.[16] The cultures were spun down (15 min × 4000*g*), and the pellet was resuspended in lysis buffer. The solution was homogenized and added dropwise to liquid nitrogen. The frozen cells were stored at −20 °C. The cells were broken by three passes through a BioNeb Cell Disruption System at 100 psi with nitrogen gas. The broken cells were removed by centrifugation (30 min × 43 500*g*). The ammonium sulfate pellet was recovered by centrifugation (10 min × 43 500*g*). The blue fractions collected from the Heparin column were exchanged using desalting columns equilibrated in 0.4 M K_2SO_4 50 mM Hepes pH 7.0. The eluent from the columns was concentrated using Pall Microsep Centrifugal Devices with 30 kDa cutoff. The purified enzyme was then stored at −60 °C.

Substrate Preparation. The substrate was prepared by irradiation of oligothymidylate solution [$p(dT)_{10}$) or $p(dT)_{14}$] (Trilink Biotechnologies, Inc.) for 180 min on ice with 254 nm light from a dual wavelength UV lamp (6 W, UV−B/UV−C, Spectroline). The formation of dimers was monitored by the decrease of the monomer absorption band at 264 nm. On the basis of the disappearance of the 264 nm absorption, we estimate the formation of about two dimers per $p(dT)_{10}$ or $p(dT)_{14}$. UV-irradiated $p(dT)_{10}$ or $p(dT)_{14}$ (UV-$p(dT)_{10}$ or UV-$p(dT)_{14}$) was not further purified because of the high affinity of photolyase for the CPD photoproduct[21] and was stored at −80 °C until ready for use.

Enzyme Activity. The enzyme activity was measured by monitoring the repair of cyclobutane pyrimidine dimers by photolyase as a function of time with 2-min intervals by using UV−vis spectroscopy following the procedure developed by Jorns et al.[40] Briefly, UV-$p(dT)_{10}$ was used as a substrate, and repair of the cyclobutane pyrimidine dimers by photolyase was followed by the reappearance of the absorption at 264 nm. The photorepair was accomplished by irradiating the mixture with 365 nm light from a dual wavelength UV lamp (6 W, UV-A/UV−B, Spectroline). The initial rate of repair was determined graphically by plotting the absorption increase due to monomerized thymine at 260 nm versus time.

Electronic Absorption and Resonance Raman Spectroscopy. The electronic absorption spectra were obtained with a Perkin-Elmer Lambda P40 UV−vis spectrometer at room temperature. The absorption spectra were deconvoluted with a set of normalized Gaussians of the form:

$$G(x) = [A/(w\sqrt{\pi/2})] \exp\{-2[(x - x_0)^2/w^2]\}$$

where A is the area, w is the width, and x_0 is the position of the Gaussian. The fitting procedure was performed with Igor Pro 4.07 (WaveMetrics, Inc.).

The resonance Raman experiments were performed on a system consisting of a single spectrograph (TriAx 550, JY/Horiba) and a N_2(l)-cooled CCD detector (Spectrum One, JY/Horiba) equipped with a UV-enhanced 2048 × 512 chip (EEV). The samples were placed in Raman spinning cells, which required 180 μL of sample containing 120 μM photolyase and were sealed with rubber septa. Excitation of the samples was done with 568.2 and 530.9 nm light from a Kr^+ ion laser (Coherent, I-302). Laser plasma lines were removed with a fused-silica Pellin-Broca prism (Lambda Research Optics, Inc.), in combination with 3-nm band-pass filters (Omega Optical). The laser light was focused onto the sample with a quartz lens of 50-mm focal length. The Raman scattered light was collected at a 90° angle with a 50 mm f/1.2, camera lens (Nikkor, Nikon). Rayleigh scattering was removed with the appropriate holographic notch filters (Kaiser Optics). The scattered light was focused into the spectrograph with a 50-mm, fused-silica lens with a focal length of 300 mm. Before entering the spectrograph, the light was passed through a wedge depolarizer (CVI Lasers Corp.) to remove polarization effects of the spectrograph and detector. The samples in the spinning cells were placed in a chamber that was cooled with nitrogen gas, which was passed through an acetone/dry ice bath. The temperature of the sample was kept at 6 ± 2 °C. The absorption spectrum of photolyase after 30 min exposure to 10 mW laser light at 6 °C was almost identical to that before the experiment. Only minimal oxidation was observed in the absorption spectrum, and no vibrations due to FAD_{ox} were observed in the resonance Raman spectra because of selective enhancement of FADH•.

Stopped-Flow Experiments. The kinetic traces were obtained with a KinTek Minimixer, which was placed in a UV−vis spectrometer (Cary 300, Varian). The mixing cuvette has a 0.5-cm optical path length with an 8-ms deadtime. The final protein concentration in the mixing cuvette was 22 μM, while that of UV-p$(dT)_{14}$ was 47 μM. The spectrometer had a bandwidth of 4 nm and an averaging time of 33 ms. The mixing cuvette was thermostated to 10 °C.

Results

After purification of photolyase, its FAD cofactor is mainly present in its neutral radical semiquinone form, but the presence of a small amount of oxidized FAD (<5%) is not always avoidable because of the sensitivity of the enzyme to oxygen. Spectroscopic experiments on *E. coli* photolyase are usually performed at high glycerol concentrations because the enzyme is more resistant to air oxidation under those conditions, and no oxidation of the FADH• is observed after storage of the enzyme at 4 °C for several weeks. Although glycerol stabilizes the enzyme, glycerol vibrations contribute significantly to resonance Raman spectra. Therefore, we have explored several different buffers for resonance Raman experiments. The best results were obtained when photolyase was exchanged into 50 mM Hepes buffer at pH 7.0 in the presence of 0.4 M K_2SO_4. Under these conditions, prolonged storage of the enzyme at −80 °C had no effect on the stability or activity of the enzyme compared to the glycerol buffer, but the enzyme was more sensitive to oxidation following prolonged storage at 4 °C. We determined the rate of repair of 5 ± 1 dimers per minute per enzyme in either buffer, which is in excellent agreement with literature values.[40]

The absorption spectrum of *E. coli* photolyase in 50 mM Hepes, pH 7.0, and 0.4 M K_2SO_4 is shown in Figure 1; it is unchanged from the spectrum obtained with the glycerol buffer system. The absorption maxima at 496, 584, and 623 nm are due to electronic transitions of FADH• and can be used for selective excitation of FADH• in the resonance Raman experiments.[12,39,41−45] The 383 nm absorption band arises from the MTHF cofactor with an underlying broad absorption band associated with FADH•.[12,19]

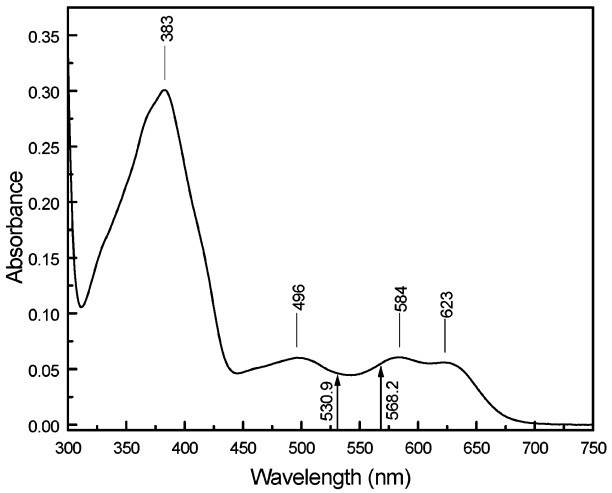

Figure 1. Absorption spectrum of *Escherichia coli* photolyase. The arrows indicate the laser excitation wavelengths that were used for the resonance Raman experiments.

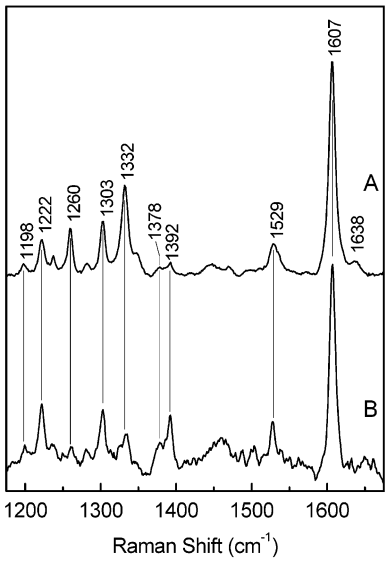

Figure 2. Resonance Raman spectra of 120 μM *E. coli* photolyase in 50 mM Hepes at pH 7 and 0.4 M K_2SO_4 excited at 530.9 nm (A) and excited at 568.2 nm (B).

To reduce the possibility of exciting either oxidized FAD or the MTHF cofactor, we have used 530.9 and 568.2 nm excitation to obtain the resonance Raman spectra of FADH• in *E. coli* photolyase, indicated with arrows in Figure 1. The resonance Raman spectra of photolyase are shown in Figure 2. The spectra show a prominent vibration with a frequency of 1607 cm^{-1} which has been recognized as a marker band for the neutral radical semiquinone flavin and has been reported to range from 1602 to 1617 cm^{-1} for various flavins and flavoproteins.[39,41−48] Other vibrations are observed at 1332, 1303, and 1260 cm^{-1}. The vibrations between 1425 and 1525 cm^{-1} are mainly associated with the Hepes buffer and could not be completely removed from the spectra by buffer subtraction. The FADH• vibrations in photolyase occur at frequencies similar to those

TABLE 1: Vibrational Frequencies (cm^{-1}) of Neutral Radical Semiquinone Flavins in Proteins

photolyase	1607	1529	1392	1378	1332	1303	1260	1222	1198	reference this work
photolyase E109A −MTHF	1605.5	1528	1391		1332	1301		1220		39
P450 reductase $FADH^{\bullet}$	1611	1540		1378		1305	1264	1226		45
P450 reductase $FMNH^{\bullet}$	1611	1532	1388			1305	1264	1227	1200	45
adrenodoxin reductase $FADH^{\bullet}$	1611				1344	1310	1271			43
flavodoxin $FMNH^{\bullet}$	1611		1391	1378	1333	1308	1269	1232		41
$RFH^{\bullet}$	1617	1533	1393				1273	1230		42

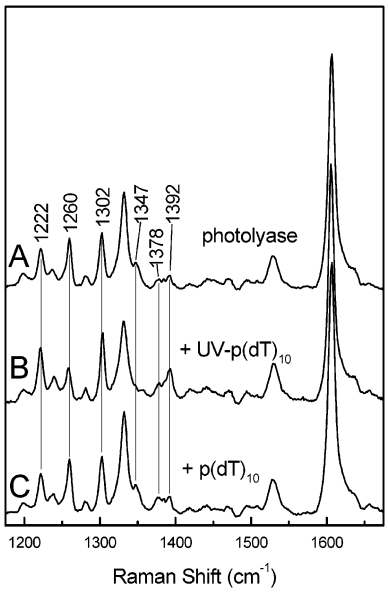

Figure 3. Resonance Raman spectra of *E. coli* photolyase (180 μM) (A), in the presence of 350 μM UV-p(dT)10 (B), and in the presence of 350 μM $p(dT)_{10}$ (C). All samples were in 50 mM Hepes, pH 7, and 0.4 M K_2SO_4.

observed for neutral radical semiquinone flavins in other proteins as listed in Table 1. The vibration at 1638 cm^{-1} is not associated with $FADH^{\bullet}$ but with the MTHF cofactor (Sokolova, O.; Schelvis, J. P. M., unpublished results).

The spectrum collected with 568.2 nm excitation shows mainly the same vibrations as those obtained with 530.9 nm excitation (Figure 2B). The most prominent changes occur in the relative intensities of the vibrations because of their Raman excitation profile. The intensities of the 1332 and 1260 cm^{-1} vibrations decrease and are enhanced upon excitation in the 496 nm absorption band, while those of the 1392, 1378, and 1222 cm^{-1} vibrations increase and are enhanced upon excitation in the 584 nm absorption band. Earlier experiments agree with this enhancement pattern.[39,41,42,44,45] The quality of the spectrum obtained with 568.2 nm is poorer because of the etaloning effect at longer wavelengths present with our back-thinned CCD detector. This spectrum is very similar to the one that was published earlier for an MTHF-less mutant of *E. coli* photolyase E109A.[39] The main difference between our data and those obtained on the MTHF-less mutant are the relative intensities of the 1378 and 1392 cm^{-1} vibrations. We observe these vibrations with a 1:2 intensity ratio for the 1378 and 1392 cm^{-1} modes, respectively, while Murgida et al. observe only the 1392 cm^{-1} vibration. This difference may be due to the mutation or the difference in MTHF content.

We collected resonance Raman spectra of photolyase in the absence and presence of substrate, UV-$p(dT)_{10}$, and the results for excitation at 530.9 nm are shown in Figure 3 (spectra A and B, respectively). Prominent changes are observed in the intensities of the vibrations at 1392, 1378, 1347, 1303, 1260, and 1222 cm^{-1} while some small but reproducible frequency

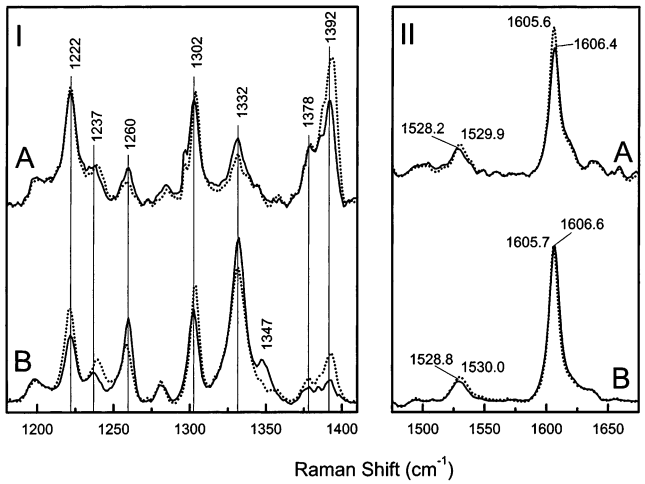

Figure 4. Changes induced in the resonance Raman spectra of *E. coli* photolyase excited at 568.2 nm (A) and 530.9 nm (B), in the absence (solid line) and presence (dotted line) of UV-$p(dT)_{10}$. Buffer conditions are the same as in Figure 3.

shifts are also observed. Figure 3 shows the control experiment of photolyase in the presence of undamaged $p(dT)_{10}$ (spectrum C), which has a resonance Raman spectrum identical to photolyase in the absence of substrate (spectrum A).

Figure 4 shows the changes in the resonance Raman spectrum of photolyase upon substrate binding in more detail for excitation at 568.2 (top) and 530.9 nm (bottom). The spectra of photolyase in the absence and presence of substrate are solid and dotted, respectively. Clearly, the changes in intensity are much stronger with 530.9 nm excitation, but both excitation wavelengths show similar frequency shifts. The largest changes in intensity are observed for the vibration at 1347 cm^{-1} which seems to disappear and the vibrations at 1222, 1237, 1302, and 1392 cm^{-1} which increase their intensity significantly. The frequency shifts range from +2.6 cm^{-1} for the 1237 cm^{-1} mode to −1.5 cm^{-1} for the 1260 cm^{-1} vibration. All changes induced by substrate binding are listed in Table 2.

Since the crystal structure of photolyase from *T. thermophilus* has been obtained with thymine bound in the substrate cavity,[28] we also measured the resonance Raman spectrum of *E. coli* photolyase in the presence of 16 mM thymine. The results are shown in Figure 5. Addition of thymine induces only one new peak in the resonance Raman spectrum of the enzyme at 1361 cm^{-1}. Control experiments with buffer containing 16 mM thymine indicate that this new vibration is due to free thymine in solution (data not shown). Therefore, we cannot detect any interaction between photolyase and thymine. This is most likely due to the very low affinity that thymine has for the photolyase substrate cavity, though we cannot rule out the possibility that thymine binding does not perturb the protein conformation or the properties of $FADH^{\bullet}$ sufficiently to cause detectable changes in its resonance Raman spectrum.

The changes in the resonance Raman spectrum that we observe upon substrate binding, that is, shifts in the vibrational frequencies and changes in the relative intensities, are most

TABLE 2: Changes in the Photolyase FADH• Vibrations on Substrate Binding and H−D Exchange

mode (cm^{-1})	frequency shift on DNA binding (cm^{-1})	intensity change on DNA binding[c] (%)	sensitive to H−D exchange
1606.5	−0.8[b]	0 (1.0)	only shoulder[a]
1528.5	+1.5[b]	+20 (1.2)	no
1391.7	+1.0[b]	+120 (2.2)	no
1378.0	0[b]	+50 (1.5)	yes
1347.3	+8[e]	−50/−65[e]	yes
1331.7	−0.4[c]	−20 (0.8)	yes
1302.5	+0.9	+30 (1.3)	yes
1259.6	−1.5	−30 (0.7)	yes
1236.7	+2.6[c]	+30 (1.3)	yes
1221.7	−0.2[b]	+50 (1.5)	yes

[a] One mode under the 1607 cm^{-1} is sensitive to the deuterium isotope. [b] Average of 568.2 and 530.9 nm data. [c] On the basis of 530.9 nm data, fold-changes are given between parentheses. [d] On the basis of 568.2 nm data. [e] The values for the 1347 cm^{-1} mode are uncertain.

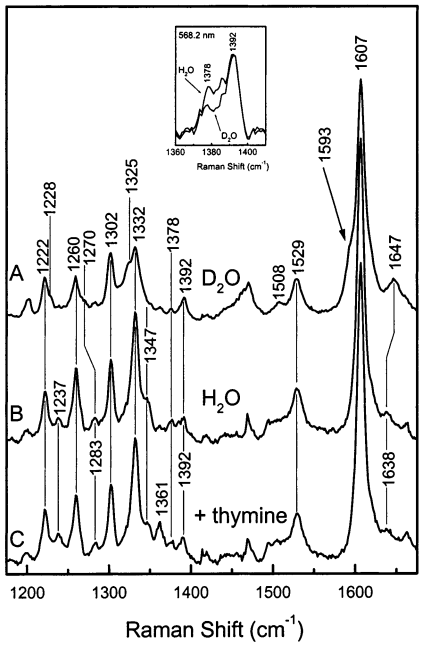

Figure 5. Resonance Raman spectra of *E. coli* photolyase excited at 530.9 nm in D_2O (A), in H_2O (B), and in H_2O in the presence of 16 mM thymine (C). Inset: 1360−1415 cm^{-1} region on excitation at 568.2 nm in H_2O (top) and D_2O (bottom). Buffer conditions are the same as in Figure 3.

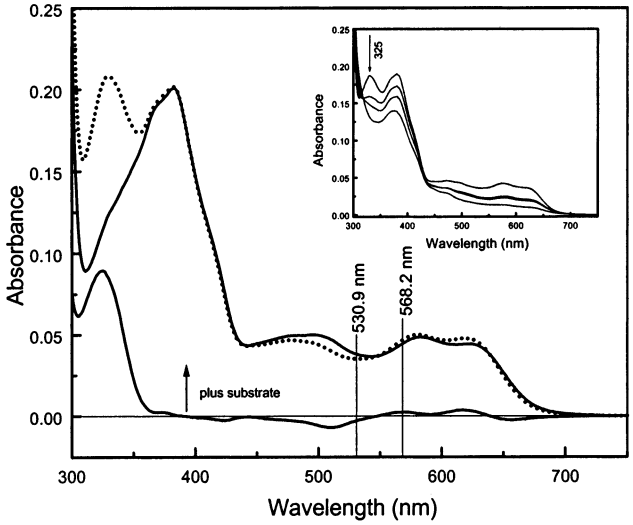

Figure 6. Absorption spectra of photolyase in the absence (solid line) and presence of UV-p$(dT)_{10}$ (dotted line). The difference spectrum (substrate-bound minus substrate-free) is shown at the bottom. The laser excitation wavelengths are indicated by the two thin lines. Inset: Photolyase with UV-p$(dT)_{10}$ in the presence of 600 μM DTT after 30 min N_2(g) purge in a sealed cuvette, after 0, 5, 10, and 15 min of irradiation with 365 nm light on ice. The arrow indicates the absorption band due to UV-p$(dT)_{10}$ and the order of the spectra after increasing irradiation time. Buffer conditions are the same as in Figure 3.

likely associated with changes in the protein environment (i.e., hydrogen bonding) of FADH•, in the Raman excitation profiles, or polarizability tensor, respectively. To determine which vibrations will be sensitive to changes in hydrogen bonding, we collected the resonance Raman spectra of photolyase in buffer containing either H_2O or D_2O. Both the N_3- and the N_5-proton of FADH• are exchangeable along with those of the amino acids that act as hydrogen-bond donors. The structure of the isoalloxazine ring of FAD and the IUPAC numbering are shown in Figure 9. The spectra are shown in Figure 5 (middle, H_2O, and top, D_2O). Almost every vibration shows sensitivity toward the H−D isotope-exchange. The 1638 cm^{-1} band shifts to 1647 cm^{-1}, and this vibration is actually associated with the MTHF cofactor (Sokolova, O.; Schelvis, J. P. M., unpublished results). One vibration moves from under the 1607 cm^{-1} band to about 1593 cm^{-1}, in agreement with the observation by Murgida et al.,[39] and a new band can be observed at 1508 cm^{-1}, which may have been obscured by buffer vibrations in the H_2O spectrum. The vibration at 1392 cm^{-1} remains unchanged while the one at 1378 cm^{-1} loses intensity. This is better observed with 568.2 nm excitation (Figure 5, inset). Other isotope sensitive vibrations and suggested isotope shifts are indicated in Figure 5. It is interesting that the vibration at 1378 cm^{-1}, which forms the main difference between photolyase in this study and the MTHF-less, E109A mutant, is sensitive to the isotope exchange. Most of the vibrations that undergo a frequency shift on substrate binding are also sensitive to H−D exchange. In addition, the 1529 cm^{-1} mode is an example of a vibration of which the frequency changes when substrate binds but is not sensitive to H−D exchange. The complete results of the effect of substrate binding and H−D exchange are given in Table 2. Since the exact shift of each vibration is not clear, we only indicate whether a vibration is sensitive to H−D exchange.

As mentioned above, the changes in Raman intensity on substrate binding can be due to changes in the Raman excitation profile or the polarizability tensor. At this stage of our research, we cannot investigate changes in the polarizability tensor, but we can investigate changes in the absorption spectrum. Figure 6 shows the absorption spectra of photolyase FADH• in the absence (solid line) and presence of UV-p$(dT)_{10}$ (dotted line) as well as the difference spectrum. The spectra show that substrate binding to photolyase induces a shift in the three visible absorption bands of FADH• to shorter wavelengths with a small increase in the extinction coefficient of the absorption bands at 632 and 584 nm and a small decrease in the extinction coefficient of the 496 nm absorption band. The large increase

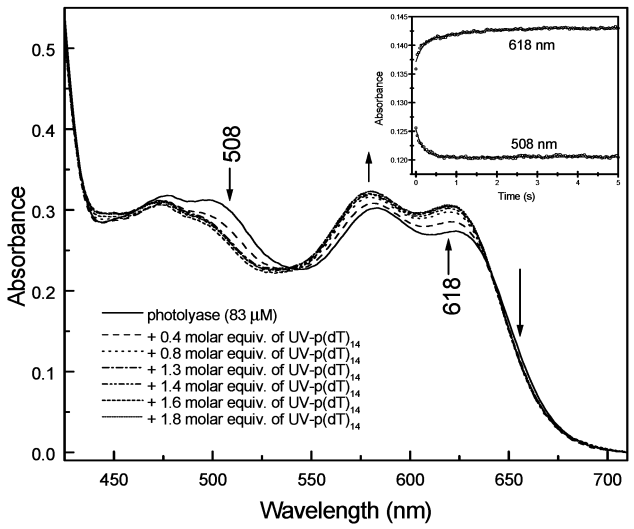

Figure 7. Absorption spectra of the titration of 83 μM photolyase with UV-p(dT)$_{14}$. The molar equivalence of UV-p(dT)$_{14}$ is given in the figure. Inset: Stopped-flow mixing experiments (open circles) of 22 μM photolyase with 2-fold excess UV-p(dT)$_{14}$ detected at 618 nm (top) and 508 nm (bottom). Each kinetic trace is the average of eight shots. The results of a global fit to the data with two exponentials having time constants of 0.17 and 1.3 s are also shown (solid line). Buffer conditions are the same as in Figure 3, and all data shown were acquired at 10° C.

in absorption at 325 nm is due to UV-p(dT)$_{10}$. The control experiment with undamaged p(dT)$_{10}$ did not change the absorption spectrum of photolyase (data not shown). The spectra in the inset show the disappearance of the 325 nm absorption band which reflects the photoconversion of some (6-4)-photoproduct to the Dewar valence dimer upon irradiation at 365 nm.[49] A large increase occurs at 264 nm (not shown) because of the repair of CPDs by functioning enzyme and the reappearance of thymine monomer absorption. The decrease in FADH$^{\bullet}$ absorption is due to its photoreduction to FADH^{-} in the presence of DTT, and the disappearance of the absorption at 383 nm is most likely due to photodecomposition of the MTHF cofactor.[19]

Further evidence that the absorption changes are induced by binding of photolyase to UV-damaged DNA is given in Figure 7. Titration of photolyase with substrate aliquots induces typical absorbance changes that level off when a stoichiometric amount of UV-p(dT)$_{14}$ has been added to photolyase. Furthermore, the inset of Figure 7 shows stopped-flow absorption data of 22 μM photolyase mixed with 2-fold excess UV-p(dT)$_{14}$. The time-dependent absorbance changes show an increase at 618 nm and a decrease at 508 nm in agreement with the titration data. A global analysis fit to exponential functions gives two time constants: 170 ms and 1.3 s. The amplitude of the 1.3 s phase is very small at 508 nm. Pseudo-first-order rate constants for photolyase binding to UV-damaged DNA of about 2×10^6 $M^{-1}s^{-1}$ have been reported by indirect methods.[50,51] At our enzyme concentration of 22 μM, this would correspond to a time constant of about 25 ms. Since our experiments were not performed under pseudo-first-order conditions, that is, >20-fold excess of substrate, it is not surprising that we measure a 7-times slower time constant. Our stopped-flow experiments are the first direct measurements of photolyase−substrate binding kinetics.

To quantify the effect of the absorption changes on the resonance Raman intensities, we transformed our absorption spectra from a wavelength to a wavenumber scale and performed a simultaneous Gaussian fit to the spectra with and without UV-p(dT)$_{10}$ present. A typical result is shown in Figure 8. The only

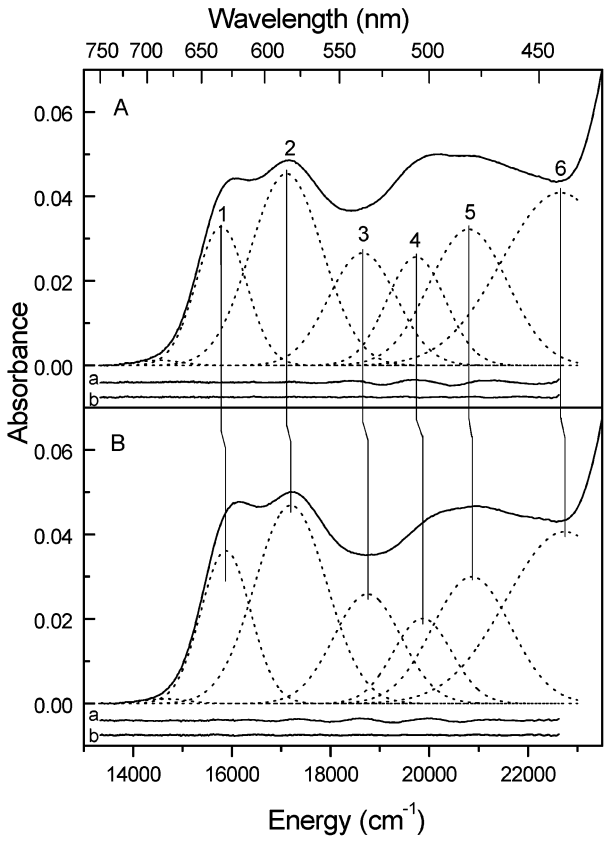

Figure 8. Deconvolution of the absorption spectrum of FADH$^{\bullet}$ in photolyase in the absence (A) and presence (B) of UV-p(dT)$_{10}$ over the range from 13333 to 22625 cm^{-1}. The dotted lines represent the normalized Gaussians that are described in Table 3. They have been labeled 1−6 for convenience. The vertical lines have been added to visualize the electrochromic shift of each band. The residuals for the fits with five (a) and six (b) Gaussians are shown at the bottom of each spectrum.

TABLE 3: Average of the Results of Curve Fitting of Six Normalized Gaussians to Three Sets of Spectra of Photolyase in the Absence (− DNA) and the Presence (+ DNA) of UV-p(dT)$_{10}$[a]

		- DNA	+ DNA	electrochromic shift
Band 1	position	15799	15885	85 ± 8
	width	985		
Band 2	position	17136	17215	79 ± 9
	width	1440		
Band 3	position	18610	18700	90 ± 10
	width	1240		
Band 4	position	19680	19788	108 ± 35
	width	1200		
Band 5	position	20778	20813	35 ± 22
	width	1625		
Band 6	position	22693	22749	55 ± 40
	width	2490		

[a] Peak positions and widths are given in cm^{-1}, and the electrochromic shift was determined by subtracting (− DNA)-data from the (+ DNA)-data.

constraint in the fit was that the widths of the corresponding absorption bands were the same in the substrate-free and substrate-bound cases. On the basis of the shape of the absorption spectra, five normalized Gaussian line shapes were initially used to describe its spectral features, that is, the peaks at 16 100 and 17 100 cm^{-1}, the peak and shoulder at 20 150 and 20 800 cm^{-1}, and a band near 23 500 cm^{-1} to provide a cutoff for the transition from FADH$^{\bullet}$ to MTHF absorption. However, the residual plots clearly indicate that a five Gaussian

TABLE 4: Relative Contributions of Bands 2, 3, and 4 to the Absorption Intensity at the Raman Excitation Wavelengths 530.9 and 568.2 nm Determined from the Gaussian Fits to the Data[a]

	Band 2			Band 3			Band 4		
	− DNA	+ DNA	change	− DNA	+ DNA	change	− DNA	+ DNA	change
530.9 nm	0.08	0.11	+38%	0.59	0.65	+10%	0.28	0.19	−32%
568.2 nm	0.85	0.89	+5%	0.14	0.10	−29%	0.01	0.01	0%

[a] These are the averages of three sets of independent experiments.

fit is not sufficient. When six Gaussians were used, the residuals became very smooth, while addition of a seventh Gaussian did not improve the fit. The results of three independent experiments are listed in Table 3. Our Gaussian deconvolution is very similar to that of oxidized flavin, which is expected given the similarities between the electronic absorption spectra of oxidized flavin and its neutral radical semiquinone.[52−54] Furthermore, the average difference between Band 1 and Band 2 is equal to 1334 ± 7 cm^{-1}, which corresponds very well to an existing vibrational mode at 1332 cm^{-1}. Although the former corresponds to an excited-state vibrational mode and the latter to one from the ground state, the energy spacing between Band 1 and Band 2 is in agreement with Band 2 being the 0−1 vibronic transition and provides evidence for the physical relevance of Bands 1 and 2 in our deconvolution. The physical origin of Band 3 is not immediately clear, but this band is very similar to Band 3 in the analysis of the absorption spectrum of the oxidized flavin and has been assigned to another vibronic band of the first electronic excited state.[52] Band 4 coincides with the absorbance maximum at 508 nm, which is the S_0-S_2 transition, while Band 5 is most likely due to a vibronic transition of the second electronic excited state. However, its proximity to the cutoff of our deconvolution makes it less reliable, and no real physical interpretation can be given to this band at this time. Band 6 was added to cover the transition region between the absorption of $FADH^•$ and MTHF and does not have any physical significance. One very small band near 14 500 cm^{-1} was needed for each deconvolution to describe the drop off of the absorption spectrum at the low-energy side, but no physical importance was given to this band. Additional experiments are underway to obtain a better understanding of the $FADH^•$ electronic absorption spectrum. However, we are very confident about the analysis of Bands 1 and 2, which was relatively independent from the number of Gaussians and method used. A global analysis (not shown) of our spectra yielded nearly identical properties for Bands 1 and 2 as those presented in Table 3. Although Bands 3 and 4 were more sensitive to the specifics of the fitting procedure (because of their proximity to the cutoff of the deconvolution), the variation in their properties is still sufficiently small to warrant a good qualitative analysis.

Our analysis indicates that the S_0-S_1 (∼633 nm or 15 800 cm^{-1}) and S_0-S_2 (∼508 nm or 19 600 cm^{-1}) transitions are almost equally affected by substrate binding with blueshifts of ∼82 cm^{-1} (average of Bands 1 and 2) and ∼108 cm^{-1}, respectively. Previous work has shown that substrate binding induces an electrochromic shift of the electronic transitions of photolyase containing FAD_{ox}, presumably because of the electric dipole moment of the CPD substrate.[35] In that study, the S_0-S_1 and S_0-S_2 transitions had a blueshift of 88 cm^{-1} and 325 cm^{-1}, respectively. The differences of the substrate electric field on FAD_{ox} and $FADH^•$ will be discussed below. On the basis of the previous work and our spectral deconvolution, we believe that the effect of substrate binding to photolyase can be explained by the electrochromic shift of the absorption spectrum, which is induced by the electric dipole moment of the substrate. An alternative explanation for the differences between the $FADH^•$ absorption spectrum in the presence and absence of substrate could be the appearance of a charge-transfer band, which is common in flavoproteins.[55−57] However, we rule out this possibility because of the observations that were mentioned above and the shape of the difference spectrum, which clearly suggests band shifts rather than the appearance of a new band. Furthermore, excitation in the charge-transfer band of flavin-substrate complexes gives rise to vibrations associated with the substrate,[55−57] but no new vibrations are observed in the resonance Raman spectra of substrate-bound photolyase.

From the curve fitting results, we were able to calculate the contribution of each absorption band at each Raman excitation wavelength. In Table 4, we show the percentage contribution of Bands 2−4 at 530.9 and 568.2 nm. Band 1 did not contribute more than 0.1% at either excitation wavelength and is not included in the analysis. Bands 5 and 6 do not contribute at 568.2 nm and their relative contributions (0.05 total) at 530.9 nm remain unchanged. It is obvious that 568.2 nm light mainly excites in Band 2, while 530.9 nm light excites $FADH^•$ in Bands 2−4. On addition of substrate, the relative contribution of Band 2 to excitation at 568.2 nm increases by about 5%, while that of Band 3 decreases by nearly 29%. On the other hand, substrate binding increases the contribution of Bands 2 and 3 at 530.9 nm by 38% and 10%, respectively, and decreases that of Band 4 by 32%. From Figure 2, we already concluded that the 1332 and 1260 cm^{-1} modes are enhanced on excitation in the 508 nm absorption band (Band 4) with 530.9 nm laser light, while the modes at 1392, 1378, 1303, and 1222 cm^{-1} are enhanced with 568.2 nm excitation in the 584 nm absorption band (Band 2). The decrease in the resonance Raman intensity of the 1332 and 1260 cm^{-1} modes on substrate binding can be attributed to the decrease in contribution of Band 4 at 530.9 nm excitation. At 568.2 nm excitation, Band 4 does not change, but Band 3 loses 29% of its contribution and is most likely the cause of the decrease in the resonance Raman intensity of the 1332 and 1260 cm^{-1} modes. This suggests that besides Band 4 also Band 3 excitation enhances these two modes but not necessarily to the same extent. The increase of the intensities of the 1392, 1378, 1303, and 1222 cm^{-1} modes is due to the increase in contribution of Band 2 at both excitation wavelengths.

Discussion

Although flavin neutral semiquinone radicals play an important role in coupling two-electron donors to one-electron acceptors, resonance Raman studies of flavoproteins have mainly focused on the oxidized form of flavin molecules, and only a small number of studies have investigated the neutral radical semiquinone form. The available resonance Raman data of neutral radical semiquinone flavins in proteins are listed in Table 1. The data on flavin neutral radical semiquinones in solution have been omitted.[47,48] A complete assignment of the normal modes of the neutral radical semiquinone flavin has yet to be reported which complicates the interpretation of the data. Spiro and co-workers pointed out that the Raman spectra of neutral radical semiquinone flavins have many similarities with those

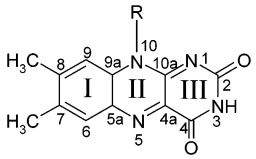

Figure 9. Structure of the isoalloxazine moiety of FAD.

of the oxidized flavin and show similar Raman excitation profiles.[41,44] Therefore, they suggested that the normal modes of the neutral radical semiquinone flavin are similar to those of the oxidized flavin but that the vibrations associated with the xylene ring (ring I, Figure 9) of the isoalloxazine moiety are not observed because of a weakened conjugation. However, a combination of later studies have indicated that ring I modes do contribute to the resonance Raman spectrum of neutral radical semiquinone flavins.[39,47,58] Recent H−D exchange and ^{15}N-isotope experiments on DNA photolyase have also shown that the Raman spectra of the neutral radical semiquinone flavin are more complex and do not strictly follow the mode assignments of the oxidized flavin.[39]

Comparison to MTHF-Free, E109A Photolyase. Comparison of our results to those of the MTHF-less, E109A mutant of *E. coli* photolyase indicates that resonance Raman spectra and, presumably, the protein-FADH$^\bullet$ interactions are very similar in MTHF-containing and MTHF-free enzyme. The main difference is that in the MTHF-less mutant only one vibration is observed at 1391 cm^{-1} while our data clearly show two vibrations at 1392 cm^{-1} and 1378 cm^{-1} with a 2:1 intensity ratio. Vibrations with similar frequencies have been reported before for flavin neutral semiquinone radicals, but the assignment of these vibrations to normal modes is not yet clear.[41,42,44,45] Spiro and co-workers suggested that the 1391 and 1378 cm^{-1} vibrations are analogous to the 1409 and 1356 cm^{-1} modes of oxidized flavin, that is, bands VI and VII, respectively, which are associated with ring I and III, and ring II modes, respectively.[41,44,59,60] Sugiyama et al. proposed that the two vibrations are both similar to band VI of oxidized flavin only with different hydrogen-bonding interactions at N_1.[45] Recently, a more precise assignment of the vibrational modes of oxidized flavins has been obtained by Zheng et al., who used density functional theory and ab initio calculations.[61] These authors have proposed that band VI consists of two overlapping modes which both have contributions from rings I and II and a methyl deformation mode. They also found evidence that band VII consists of three overlapping modes with the following structures: (i) ring I, II, and III stretch and N_{10}–$C_{1'}$ (ribityl) stretch, (ii) N_3−H bend, and (iii) ring I, II, and III stretch and N_3−H bend. If bands VI and VII of oxidized flavin correspond to the 1392 and 1378 vibrational modes of FADH$^\bullet$, respectively, then the ^{15}N-labeling and H−D exchange experiments by Murgida et al.[39] and our H−D exchange results are in agreement with the refined assignments of Zheng et al.[61] However, only isotope experiments in combination with computational methods on the neutral radical semiquinone of flavin will provide a definite answer to this problem. Therefore, in the remainder of our discussion, we will use the assignment of Murgida et al. who propose the contribution of a C−N_{10} stretch to the 1392 cm^{-1} mode of FADH$^\bullet$ in photolyase.[39]

In photolyase, the 1392 cm^{-1} vibration is not sensitive to H−D exchange, unlike the 1378 cm^{-1} vibration (Figure 5).[39] Therefore, we rule out that these two vibrations are due to the same normal mode. If these two different modes are related to the MTHF content of the two samples, the 1378 cm^{-1} vibration may be a marker band for MTHF content. The lack of the H−D sensitive vibration in the MTHF-less mutant suggests that removal of MTHF results in a loss or change of a hydrogen bond to FADH$^\bullet$. Therefore, we propose that MTHF may play a structural role by stabilizing the protein environment of the FAD cofactor. In light of the refined mode assignment for oxidized flavin and the potential similarity of the 1378 cm^{-1} mode to band VII, this stabilizing interaction may involve the N_3 hydrogen. On the basis of the $A_{380}/A_{580} = 5.0$ absorption ratio, we estimate that at least 66% of the photolyase in our sample has MTHF-bound.[62] We are currently conducting experiments to investigate the effect of MTHF content on the resonance Raman spectrum of FADH$^\bullet$ in photolyase.

Comparison to Other Flavoproteins. The vibrational frequencies of FADH$^\bullet$ in photolyase are compared to those measured for neutral radical semiquinones in other flavoproteins in Table 1. The most prominent difference between photolyase and the other flavoproteins is the frequency of the redox characteristic vibration. We observe this vibration at 1607 cm^{-1}, slightly higher than Murgida et al., and it has a frequency of 1611 cm^{-1} for FMNH$^\bullet$ and FADH$^\bullet$ containing proteins and of 1617 cm^{-1} for RFH$^\bullet$ in RBP.[39,41−45] It has been reported at 1602 cm^{-1} for FADH$^\bullet$ in glucose oxidase,[46] but we found that frequency at 1611 cm^{-1} (Schelvis, J. P. M.; Goyal, N.; Pun, D., unpublished results). Except for the vibrations at 1392 and 1378 cm^{-1}, the vibrations of FADH$^\bullet$ between 1615 and 1150 cm^{-1} all have a lower frequency in photolyase compared to neutral radical semiquinones in other flavoproteins. A decrease in flavin vibrational frequencies in proteins compared to flavins in solution has been interpreted as arising from strong hydrogen-bonding interactions with the protein.[41,60,63] Therefore, the lower vibrational frequencies of FADH$^\bullet$ in photolyase are most likely indicative of a stronger hydrogen-bonding environment of the FAD cofactor in photolyase than in other flavoproteins. The crystal structure of *E. coli* photolyase reveals several hydrogen bonds to the isoalloxazine ring of FADH$^\bullet$.[26] Most notably, the 2′-OH of the ribityl chain is within hydrogen-bonding distance of N_1. This hydrogen bond is probably formed because of the unique U-shaped structure of the FAD cofactor in photolyase. Furthermore, the C_2 carbonyl can accept hydrogen bonds from water molecules (#33 and #211), N_3−H can donate a hydrogen bond to the carboxylate group of Asp372, the C_4 carbonyl can accept a hydrogen bond from the Asp374 amide proton, and N_5–H can donate a hydrogen bond to the carbonyl group of Asn378.

Not all of the lower vibrational frequencies of FADH$^\bullet$ in photolyase can be explained by an increase in hydrogen-bonding strength. The 1607 and 1529 cm^{-1} modes are both lower in frequency than in other flavoproteins, but these modes are not sensitive to H−D exchange. Although the vibration at 1593 cm^{-1} moves from underneath the 1607 cm^{-1} band in the D_2O spectrum, this band is too weak to explain the difference of 4 cm^{-1} between the 1607 cm^{-1} mode in photolyase and in other flavoproteins. Both the 1607 and the 1529 cm^{-1} mode have been suggested to originate from ring II.[44] However, Murgida et al. showed that the 1529 cm^{-1} mode is sensitive to ^{15}N labeling and proposed that it contains contributions from C−C and C−N_5,[39] which supports the assignment of this mode to rings I and II by Su and Tripathi.[47] They also observed ^{15}N sensitivity of one of the two modes at 1605.5 cm^{-1}. Therefore, they assigned the ^{15}N sensitive mode to a contribution of C−C and C−N_5 and N_5–H (bending) and the nonsensitive mode to C_{5a}−C_{9a} and C_{10a}−C_{4a}. However, Nishina et al. have reported that the 1617 cm^{-1} mode of RFH$^\bullet$ in RBP and the 1602 cm^{-1} mode of FAD$^{\bullet-}$ in D-amino acid oxidase are not sensitive to

isotopic substitution of C_2, C_{4a}, C_4, C_{10a}, N_5, N_1, and N_3, and they assigned these vibrations to ring I.[57] Furthermore, the substitution of the C_8 methyl group with a methoxy group splits the RFH• 1617 cm^{-1} mode in two new modes at 1623 and 1615 cm^{-1}, of which only the 1615 cm^{-1} mode is sensitive to H−D exchange.[42] This is very similar to the H−D exchange behavior of the 1607 cm^{-1} mode of FADH• in photolyase and indicates that one 1617 cm^{-1} mode (the strong 1607 cm^{-1} mode of FADH•) is sensitive to ring I substitution but not to H−D exchange, while the other is not sensitive to ring I substitution but is sensitive to H−D exchange. Therefore, we favor the assignment of Su and Tripathi that the non H−D sensitive 1607 cm^{-1} mode is due to C═C stretching of ring I with a strong contribution from $C_{5a}C_{9a}$.[47] For the ^{15}N and H−D sensitive 1607 cm^{-1} mode, we will follow the assignment of Murgida et al.,[39] that is, a C−C, C−N_5, and N_5–H (bending) mode, which is mainly located on ring II with a contribution from ring I.

EPR spectroscopy of FADH• in photolyase has shown that the radical spin density is more localized in photolyase than in other flavoproteins.[64,65] The electron density seems to be strongly affected by hydrogen bonding and is mainly localized on atoms that appear to be involved in the modes describing the 1607 and 1529 cm^{-1} vibrations. This additional electron density in their bonds may result in a reduction of the overall bond order of these normal modes and a lowering of their vibrational frequencies. Therefore, the lower vibrational frequency of these two vibrations, especially of the 1607 cm^{-1} mode, may be a manifestation of the localized radical spin density and related to the unique stability of FADH• in photolyase.

The Effects of Substrate Binding. The titration and stopped-flow data (Figure 7) show unambiguously that the observed spectroscopic changes of FADH• are due to the formation of the photolyase−substrate complex. Our analysis of the absorption spectra of photolyase in the absence and presence of UV-$p(dT)_{10}$ (Tables 3 and 4) indicates that the electric dipole moment of the CPD induces electrochromic shifts of the transition dipole moments of FADH• similar to those in FAD_{ox}.[35] Besides changes in the electronic transition energies, there are also changes in the extinction coefficients for the different transitions. Although the electrochromic shift can be used to predict geometric properties of the photolyase−substrate complex (see below), it does not provide information about possible perturbations of the active site on substrate binding. However, changes in the vibrational spectra of FADH• can reveal such information.

The resonance Raman spectrum of photolyase shows changes in Raman intensities and in vibrational frequencies on substrate binding. Since both intensity changes and frequency shifts show changes in opposite directions for different vibrations, we rule out that these observations are due to an artifact. The changes in Raman intensities can be largely explained by changes in the Raman excitation profiles because of the electrochromic shift. At 568.2 nm, substrate binding results in a 5% increase of excitation in Band 2 and a 29% decrease of excitation in Band 3. These calculations explain very well the small increase in intensities of the 1222, 1237, and 1302 cm^{-1} vibrations and the significant decrease in those of the 1260 and 1332 cm^{-1} modes in agreement with enhancement on excitation in Band 2 and Band 3, respectively. Since Band 4 does not contribute to the absorbance at 568.2 nm, this band cannot be responsible for the decrease in intensity of the modes at 1260 and 1332 cm^{-1} at this excitation wavelength. At 530.9 nm, addition of UV-$p(dT)_{10}$ results in a 38% and a 10% increase of excitation in Bands 2 and 3, respectively, and a 32% decrease of excitation in Band 4. The increase in contribution of Band 2 absorption at 530.9 nm excitation is in agreement with the assignment of its enhancement of the 1222, 1237, and 1302 cm^{-1} vibrations. The small increase in the absorption of Band 3 at this wavelength cannot explain the decrease in the intensity of the 1260 and 1332 cm^{-1} modes. Therefore, Band 4, whose intensity decreases significantly at 530.9 nm on substrate binding, is the only band that can be responsible for the observed decrease in intensity of these two modes. We propose that both Band 3 and Band 4 give rise to enhancement of the 1260 and 1332 cm^{-1} modes. To explain the 20−30% decrease in their intensity, their enhancement has to be more significant on excitation in Band 4 than in Band 3. We conclude that the electrochromic shift of the FADH• absorption bands on substrate binding changes the Raman excitation profiles and provides a very good qualitative account of the changes in resonance Raman intensities.

Two vibrational modes form exceptions: the 1347 and 1392 cm^{-1} vibrations. The 1347 cm^{-1} vibration loses more than 50% of its intensity, instead of 32%, and may be shifting to a higher frequency. The 1392 cm^{-1} mode shows the expected enhancement on an increase of Band 2 excitation, but its enhancement is anomalous, about 50% instead of 5% and 120% instead of 38% on 568.2 and 530.9 nm excitation, respectively. These discrepancies may be due to the poor current knowledge of the Raman excitation profiles of FADH• or to changes in the polarizability tensor of FADH• induced by the substrate electric dipole moment. Detailed analysis of Raman excitation profiles and the electric field effect on the polarizability tensor is outside the scope of the current paper and will be investigated soon.

The frequency shifts induced by substrate binding to photolyase range from +2.6 to −1.5 cm^{-1} which is within the range for changes in hydrogen-bonding interactions.[60] Therefore, the observed frequency shifts on binding of substrate to photolyase may be primarily due to changes in the hydrogen-bonding interaction between FADH• and its protein environment. This conclusion is supported by the H−D isotope sensitivity of most of these vibrations and indicates that substrate binding may perturb the photolyase active site slightly. However, the vibrations at 1607, 1529, and 1392 cm^{-1} are not sensitive to H−D exchange but still display reproducible frequency shifts on substrate binding. We propose that this is due to the vibrational Stark effect (VSE) induced by the electric dipole moment of the substrate. The electric dipole can affect the order of a bond depending on its orientation with respect to the bond. VSE has recently been measured for carbonyl and nitrile vibrations using FTIR spectroscopy, and changes in vibrational frequencies in recent surface-enhanced Raman experiments were also explained by VSE.[66−68] On the basis of a computer model of the photolyase−substrate complex, it is proposed that a projection of the substrate electric field onto the isoalloxazine plane lies along the N_{10}–C_{10a} bond.[30,35] Comparison of the proposed normal mode structure of the 1607, 1529, and 1392 cm^{-1} vibrations shows that the 1529 and 1392 cm^{-1} modes have contributions from C−N_5 and C−N_{10}, respectively, and that ring I C═C stretching contributes to the 1607 cm^{-1} vibration with a significant involvement of C_{5a}−C_{9a}.[47] The 1529 and 1392 cm^{-1} modes contain at least one bond parallel to the projection of the electric field vector, that is, C_{4a}−N_5 and N_{10}–C_{10a}, respectively, suggesting that they will be subject to the VSE. Furthermore, the frequency of these two modes increases, suggesting that the weighted bond order of these normal modes increases in the presence of the electric field. In the 1607 cm^{-1} vibration, a component of the projection of the electric field

vector lies along the $C_{5a}-C_{9a}$ bond, which is thought to be the principal contributor to this mode,[47] and it shifts to a lower frequency in the presence of the electric field indicating a decrease in the weighted bond order of the mode. The normal mode structure of the other vibrations is less clear, and the effect of the electric field on their frequencies cannot be analyzed at this point. We do expect that the VSE also contributes to the frequency changes in these vibrations in addition to changes in hydrogen bonding. The frequency shift of the 1237 cm^{-1} vibration ($+2.6$ cm^{-1}) and the possible $+8$ cm^{-1} shift of the 1347 cm^{-1} mode on substrate binding seem too large to be explained by VSE, and we propose that these vibrations, which are also sensitive to H−D exchange, are indicative of small perturbations of the protein hydrogen-bonding environment of $FADH^{\bullet}$ on substrate binding. Without detailed knowledge of the normal coordinate structure of $FADH^{\bullet}$, we cannot indicate which hydrogen bonds are affected. Our observations can be explained by the effect of the electric dipole moment of the CPD on $FADH^{\bullet}$ and by small perturbations of the hydrogen-bonding environment of $FADH^{\bullet}$ on substrate binding by photolyase.

Geometry of the Photolyase−Substrate Complex. MacFarlane and Stanley showed that the electric dipole moment of the CPD is responsible for the electrochromic shift of the electronic transition energies of FAD_{ox} in photolyase.[35] They reported blueshifts of 88 and 325 cm^{-1} for the S_0-S_1 and the S_0-S_2 transitions of FAD_{ox}, respectively. The electrochromic shift (ΔE, in cm^{-1}) is given by:[69]

$$\Delta E = -\frac{\Delta\vec{\mu}_n \cdot \vec{F}_{CPD}}{hc} = -\frac{|\Delta\vec{\mu}_n||\vec{F}_{CPD}|\cos\gamma}{hc} \qquad (1)$$

where $\Delta\vec{\mu}_n$ is the difference dipole moment of the chromophore ($\Delta\vec{\mu}_n = \vec{\mu}_n - \vec{\mu}_0$, where n indicates the nth excited state), $\vec{F}_{CPD}$ is the electric field of the CPD photoproduct at the chromophore, γ is the angle between the two vectors, h is Planck's constant, and c is the speed of light. Since $\Delta\vec{\mu}_n$ has been determined for FAD_{ox}, MacFarlane and Stanley could use the electrochromic shift of FAD_{ox} in photolyase,[35] the point-dipole approximation for $\vec{F}_{CPD}$, and additional information from a photolyase−substrate computer model[30] to estimate the geometry of the CPD−FAD_{ox} complex, that is, γ and r, which is the distance between CPD and FAD_{ox} and comes from the point-dipole approximation.[35] They concluded that the CPD binds in the substrate cavity at a distance between 5.5 and 8 Å from FAD_{ox} with $\gamma = 141°$ and 165° for $\Delta\vec{\mu}_1$ and $\Delta\vec{\mu}_2$, respectively.

Unfortunately, $\Delta\vec{\mu}_n$ is not known for $FADH^{\bullet}$, and we cannot calculate these parameters for $FADH^{\bullet}$. The fact that we measure a similar blueshift for $FADH^{\bullet}$ as has been reported for FAD_{ox} in photolyase suggests that the orientation and distance of the CPD with respect to $FADH^{\bullet}$ is also similar as for FAD_{ox}. This is not too surprising since we do not expect that the protein will have a significantly different conformation depending on the redox state of the FAD cofactor, and this would also mean that $\Delta\vec{\mu}_1$ is very similar for $FADH^{\bullet}$ and FAD_{ox}. Eaton et al. determined that the orientation of the S_0-S_1 and S_0-S_2 transition dipole moments of $FMNH^{\bullet}$ in flavodoxin are almost identical to those of FMN_{ox}.[54] They suggested that the extra H-atom at N_5 affects the transition dipole energies but not their orientation. Therefore, it is possible that electric dipole moments of $FADH^{\bullet}$ in the S_0 and S_1 states are very similar to those in FAD_{ox}, resulting in a very similar $\Delta\vec{\mu}_1$. If the geometry of the CPD−FAD complex is independent of the redox state of FAD, the electrochromic shift of $\sim$108 cm^{-1} for the S_0 to S_2 transition suggests that $\Delta\vec{\mu}_2$ in $FADH^{\bullet}$ is significantly different from that in FAD_{ox}. Since $\Delta\vec{\mu}_1$ is very similar in the two redox states, it seems that $\vec{\mu}_0$ and $\vec{\mu}_1$ have to be very similar also. Therefore, the difference in $\Delta\vec{\mu}_2$ and in the electrochromic shift is most likely due to a different orientation or magnitude of $\vec{\mu}_2$ in $FADH^{\bullet}$ compared to FAD_{ox}. The results on FAD_{ox} were obtained using FAD-reconstituted apoprotein. Since the S_0-S_2 transition of FAD is much more sensitive to protein environment than the S_0-S_1 transition, it is possible that the larger electrochromic shift of the S_0-S_2 transition for FAD_{ox} is partially due to a slight misalignment of the FAD cofactor after reconstitution which is corrected upon substrate binding. Determination of the difference dipole moments of $FADH^{\bullet}$ in photolyase could provide further insight into this issue.

Conclusions

Our results show that substrate binding to unmanipulated *E. coli* photolyase induces changes in both the resonance Raman and the absorption spectrum of $FADH^{\bullet}$. The electrochromic shift of $\sim$82 cm^{-1} observed in the latter case is in good agreement with that observed in FAD-reconstituted photolyase which suggests that the substrate binding geometry is similar. The changes in resonance Raman intensities that are observed on substrate binding can largely be explained by the electrochromic shift of the $FADH^{\bullet}$ electronic transitions which cause a change in the Raman excitation profiles of the $FADH^{\bullet}$ vibrations. The frequency shifts that are observed on substrate binding can be explained by the vibrational Stark effect of the electric dipole moment of the substrate on the $FADH^{\bullet}$ vibrations and by small perturbations of the protein environment of $FADH^{\bullet}$, that is, changes in hydrogen bonds. This suggests that substrate binding slightly alters the photolyase active site.

The resonance Raman spectrum of the MTHF-containing photolyase in our study contains one H−D sensitive vibration that is not observed in the MTHF-free mutant E109A photolyase. We propose that this vibration indicates that removal of MTHF affects hydrogen bonding to $FADH^{\bullet}$, and MTHF may have a structural role in stabilizing the photolyase active site. Comparison of the photolyase $FADH^{\bullet}$ resonance Raman spectra to those of neutral radical semiquinones in other flavoproteins indicates that $FADH^{\bullet}$ is in a strong hydrogen-bonding environment in photolyase.

Finally, we demonstrated that the electrochromic shift induced by substrate binding can be used to study the binding kinetics of photolyase and its substrate with stopped-flow techniques. We are starting a systematic investigation of the binding kinetics to determine the mode of damage recognition by photolyase.

References and Notes

(1) Görner, H. *J. Photochem. Photobiol., B* **1994**, *26*, 117−139.
(2) Perdiz, D.; Gróf, P.; Mezzina, M.; Nikaido, O.; Moustacchi, E.; Sage, E. *J. Biol. Chem.* **2000**, *275*, 26732−26742.
(3) Husain, I.; Griffith, J.; Sancar, A. *Proc. Natl. Acad. Sci. U.S.A.* **1988**, *85*, 2558−2562.
(4) McAteer, K.; Jing, Y.; Kao, J.; Taylor, J.-S.; Kennedy, M. A. *J. Mol. Biol.* **1998**, *282*, 1013−1032.
(5) Park, H.; Zhang, K.; Ren, Y.; Nadji, S.; Sinha, N.; Taylor, J.-S.; Kang, C. *Proc. Natl. Acad. Sci. U.S.A.* **2002**, *99*, 15965−15970.
(6) You, Y.-H.; Lee, D.-H.; Yoon, J.-H.; Nakajima, S.; Yasui, A.; Pfeirer, G. P. *J. Biol. Chem.* **2001**, *276*, 44688−44694.
(7) Vink, A.; Roza, L. *J. Photochem. Photobiol., B* **2001**, *65*, 101−104.
(8) Sancar, A. *Biochemistry* **1994**, *33*, 2−9.
(9) Yasui, A.; Eker, A. P. M. In *DNA Damage and Repair, Vol. 2: DNA Repair in Higher Eukaryotes*; Nickoloff, J. A., Hoekstra, M. F., Eds.; Humana Press Inc.: Totowa, NJ, 1998; pp 9−32.
(10) Todo, T. *Mutat. Res.* **1999**, *434*, 89−97.
(11) Sancar, A.; Smith, F. W.; Sancar, G. B. *J. Biol. Chem.* **1984**, *259*, 6028−6032.

(12) Jorns, M. S.; Sancar, G. B.; Sancar, A. *Biochemistry* **1984**, *23*, 2673−2679.
(13) Johnson, J. L.; Hamm-Alvarez, S.; Payne, G.; Sancar, G. B.; Rajagopalan, K. V.; Sancar, A. *Proc. Natl. Acad. Sci. U.S.A.* **1988**, *85*, 2046−2050.
(14) Sancar, G. B.; Smith, F. W.; Sancar, A. *Nucleic Acids Res.* **1983**, *11*, 6667−6678.
(15) Okamura, T.; Sancar, A.; Heelis, P. F.; Begley, T. P.; Hirata, Y.; Mataga, N. *J. Am. Chem. Soc.* **1991**, *113*, 3143−3145.
(16) Gindt, Y. M.; Vollenbroek, E.; Westphal, K.; Sackett, H.; Sancar, A.; Babcock, G. T. *Biochemistry* **1999**, *38*, 3857−3866.
(17) Aubert, C.; Vos, M. H.; Mathis, P.; Eker, A. P. M.; Brettel, K. *Nature* **2000**, *405*, 586−590.
(18) Li, Y. F.; Heelis, P. F.; Sancar, A. *Biochemistry* **1991**, *30*, 6322−6329.
(19) Heelis, P. F.; Payne, G.; Sancar, A. *Biochemistry* **1987**, *26*, 4634−4640.
(20) Sancar, G. B. *Mutat. Res.* **2000**, *451*, 25−37.
(21) Husain, I.; Sancar, A. *Nucleic Acids Res.* **1987**, *15*, 1109−1120.
(22) Sancar, G. B.; Smith, F. W.; Sancar, A. *Biochemistry* **1985**, *24*, 1849−1855.
(23) Husain, I.; Sancar, G. B.; Holbrook, S. R.; Sancar, A. *J. Biol. Chem.* **1987**, *262*, 13188−13197.
(24) Baer, M. E.; Sancar, G. B. *J. Biol. Chem.* **1993**, *268*, 16717−16724.
(25) Kim, S.-T.; Sancar, A. *Biochemistry* **1991**, *30*, 8623−8630.
(26) Park, H.-W.; Kim, S.-T.; Sancar, A.; Deisenhofer, J. *Science* **1995**, *268*, 1866−1872.
(27) Tamada, T.; Kitadokoro, K.; Higuchi, Y.; Inaka, K.; Yasui, A.; de Ruiter, P. E.; Eker, A. P. M.; Miki, K. *Nat. Struct. Biol.* **1997**, *4*, 887−891.
(28) Komori, H.; Masui, R.; Kuramitsu, S.; Yokoyama, S.; Shibata, T.; Inoue, Y.; Miki, K. *Proc. Natl. Acad. Sci. U.S.A.* **2001**, *98*, 13560−13565.
(29) Vande Berg, B. J.; Sancar, G. B. *J. Biol. Chem.* **1998**, *273*, 20276−20282.
(30) Sanders, D. B.; Wiest, O. *J. Am. Chem. Soc.* **1999**, *121*, 5127−5134.
(31) Hahn, J.; Michel-Beyerle, M.-E.; Rösch, N. *J. Phys. Chem. B* **1999**, *103*, 2001−2007.
(32) Antony, J.; Medvedev, M.; Stuchebruhkov, A. A. *J. Am. Chem. Soc.* **2000**, *122*, 1057−1065.
(33) Weber, S.; Richter, G.; Schleicher, E.; Bacher, A.; Mobius, K.; Kay, C. W. M. *Biophys. J.* **2001**, *81*, 1195−1204.
(34) Jorns, M. S.; Wang, B.; Jordan, S. P.; Chanderkar, L. P. *Biochemistry* **1990**, *29*, 552−561.
(35) MacFarlane, A. W., IV.; Stanley, R. J. *Biochemistry* **2001**, *40*, 15203−15214.
(36) Christine, K. S.; MacFarlane, A. W.; Yang, K.; Stanley, R. J. *J. Biol. Chem.* **2002**, *277*, 38339−38344.
(37) Morris, M. D.; Bienstock, R. J. In *Advances in Spectroscopy* Vol. 13: *Spectroscopy of Biological Systems*; Clark, R. J. H., Hester, R. E., Eds.; Wiley & Sons: New York, 1986; pp 395−442.
(38) McFarland, J. T. In *Biological Applications of Raman Spectroscopy* Vol. 2: *Resonance Raman Spectra of Polyenes and Aromatics*; Spiro, T. G., Ed.; Wiley: New York, 1987; pp 211−302.
(39) Murgida, D. H.; Schleicher, E.; Bacher, A.; Richter, G.; Hildebrandt, P. *J. Raman Spec.* **2001**, *32*, 551−556.
(40) Jorns, M. S.; Sancar, G. B.; Sancar, A. *Biochemistry* **1985**, *24*, 1856−1861.
(41) Dutta, P. K.; Spiro, T. G. *Biochemistry* **1980**, *19*, 1590−159.
(42) Nishina, Y.; Shiga, K.; Horiike, K.; Tojo, H.; Kasai, S.; Matsui, K.; Watari, H.; Yamano, T. *J. Biochem.* **1980**, *88*, 411−416.
(43) Kitagawa, T.; Sakamoto, H.; Sugiyama, T.; Yamano, T. *J. Biol. Chem* **1982**, *257*, 12075−12080.
(44) Benecky, M. J.; Copeland, R. A.; Spiro, T. G. *Biochim. Biophys. Acta* **1983**, *760*, 163−168.
(45) Sugiyama, T.; Nisimoto, Y.; Mason, H. S.; Loehr, T. M. *Biochemistry* **1985**, *24*, 3012−3019.
(46) Lively, C. R.; Gustafson, W. G.; McFarland, J. T. In *Flavins and Flavoproteins*; Edmondson, D. E., McCormick, D. B., Eds.; W. de Gruyter & Co.: Berlin, 1987; pp 283−286.
(47) Su, Y.; Tripathi, G. N. R. *J. Am. Chem. Soc.* **1994**, *116*, 4405−4407.
(48) Sakai. M.; Takahashi, H. *J. Mol. Struct.* **1996**, *379*, 9−18.
(49) Taylor, J. S. *Acc. Chem. Res.* **1994**, *27*, 76−82.
(50) Harm, W. *Mutat. Res.* **1970**, *10*, 277−290.
(51) Sancar, G. B.; Smith, F. W.; Reid, R.; Payne, G.; Sancar, A. *J. Biol. Chem.* **1987**, *262*, 478−485.
(52) Edmondson, D. E.; Tollin, G. *Biochemistry* **1971**, *10*, 113−124.
(53) Shiga, K.; Nishina, Y.; Ohmine, I.; Horiike, K.; Kasai, S.; Matsui, K.; Watari, H.; Yamano, T. *J. Biochem.* **1980**, *87*, 281−287.
(54) Eaton, W. A.; Hofrichter, J.; Makinen, M. W.; Andersen, R. D.; Ludwig, M. L. *Biochemistry* **1975**, *14*, 2146−2151.
(55) Nishina, Y.; Kitagawa, T.; Shiga, K.; Watari, H.; Yamano, T. *J. Biochem.* **1980**, *87*, 831−839.
(56) Zheng, Y.; Massey, V.; Schaller, A.; Palfey, B. A.; Carey, P. R. *J. Raman Spectrosc.* **2001**, *32*, 579−586.
(57) Nishina, Y.; Shiga, K.; Miura, R.; Tojo, H.; Ohta, M.; Miyake, Y.; Yamano, T.; Watari, H. *J. Biochem.* **1983**, *94*, 1979−1990.
(58) Nishina, Y.; Tojo, H.; Shiga, K. *J. Biochem.* **1988**, *104*, 227−231.
(59) Bowman, W. D.; Spiro, T. G. *Biochemistry* **1981**, *20*, 3313−3318.
(60) Lively, C. R.; McFarland, J. T. *J. Phys. Chem.* **1990**, *94*, 3980−3994.
(61) Zheng, Y.; Dong, J.; Palfey, B. A.; Carey, P. R. *Biochemistry* **1999**, *38*, 16727−16732.
(62) Wang, B.; Jorns, M. S. *Biochemistry* **1989**, *28*, 1148−1152.
(63) Irwin, R. M.; Visser, A. J. W. G.; Lee, J.; Carreira, L. A. *Biochemistry* **1980**, *19*, 4639−4646.
(64) Kay, C. W. M.; Feicht, R.; Schulz, K.; Sadewater, P.; Sancar, A.; Bacher, A.; Möbius, K.; Richter, G.; Weber, S. *Biochemistry* **1999**, *38*, 16740−16748.
(65) Weber, S.; Möbius, K.; Richter, G.; Kay, C. W. M. *J. Am. Chem. Soc.* **2001**, *123*, 3790−3798.
(66) Andrews, S. S.; Boxer, S. G. *J. Phys. Chem. A* **2000**, *104*, 11853−11863.
(67) Park, E. S.; Boxer, S. G. *J. Phys. Chem. B* **2002**, *106*, 5800−5806.
(68) Oklejas, V.; Sjostrom, C.; Harris, J. M. *J. Am. Chem. Soc.* **2002**, *124*, 2408−2409.
(69) Liptay, W. *Angew. Chem., Int. Ed. Engl.* **1969**, *8*, 177−188.